Electrical Power and Energy Systems 86 (2017) 81–92

Contents lists available at ScienceDirect

Electrical Power and Energy Systems

journal homepage: www.elsevier.com/locate/ijepes

Control and protection sequence for recovery and reconfiguration of an offshore integrated MMC multi-terminal HVDC system under DC faults

Puyu Wang [a,b], Xiao-Ping Zhang [b,*], Paul F. Coventry [c], Ray Zhang [c], Zhou Li [d]

[a] Department of Electrical Engineering, School of Automation, Nanjing University of Science and Technology, Nanjing, Jiangsu 210094, China
[b] Department of Electronic, Electrical and Systems Engineering, School of Engineering, College of Engineering Physical Sciences, University of Birmingham, Edgbaston, Birmingham B15 2TT, United Kingdom
[c] National Grid, National Grid House, Warwick Technology Park, Gallows Hill, Warwick CV34 6DA United Kingdom
[d] School of Electrical Engineering, Southeast University, Nanjing, Jiangsu 210096, China

ARTICLE INFO

Article history:
Received 1 December 2015
Received in revised form 7 September 2016
Accepted 13 October 2016
Available online 28 October 2016

Keywords:
DC fault
Control and protection sequence
Recovery and reconfiguration sequence
Multi-terminal HVDC (MTDC)
Modular multilevel converter (MMC)
Offshore wind farm (OWF)
Master-slave control
Droop control

ABSTRACT

A comprehensive process of the control and protection against a DC fault in a voltage source converter (VSC) based high-voltage direct current (HVDC) system typically includes fault detection, fault isolation and system recovery. Regarding an offshore wind farm (OWF) integrated modular multilevel converter (MMC) based multi-terminal HVDC (MTDC) system with two control paradigms, i.e. master-slave control and droop control under DC faults, this paper presents the fault isolation, including the isolation of the faulted line section, with detailed control and protection sequence, which would be useful for practical engineering. The control and protection sequence at the system recovery/reconfiguration phase is comprehensively investigated, which includes: (1) when to start the recovery/reconfiguration control; (2) the sequence between deblocking the MMCs and reclosing the AC circuit breakers (AC CBs); and (3) the recovery sequence of each HVDC terminal. Based on the analysis of the system characteristics, a preferred recovery/reconfiguration scheme is proposed. Simulation results on the real-time digital simulator (RTDS) validate the proposed scheme and demonstrate the advantages through comparison with a different recovery sequence. The impact of transient and permanent DC faults on the system recovery/reconfiguration control is discussed. In addition, the recovery/reconfiguration control of the MTDC in radial and meshed topologies is compared and demonstrated. Based on the analytical and simulation studies, a general guideline on the recovery/reconfiguration control of MMC MTDC systems is proposed.

1. Introduction

Intensive research has been conducted on the control and protection against DC faults for the VSC based HVDC grids. Generally, a complete process of control and protection against a fault comprises 3 phases [1,2]: fault detection, fault isolation and system recovery/reconfiguration, as illustrated in Fig. 1.

The fault detection at Phase 1 consists of detecting and locating the fault based on the fault characteristics. Some researchers proposed solutions for detecting and locating DC faults in a VSC MTDC grid [3,4]. The fault isolation at Phase 2 comprises isolating the fault by associated protective action and then isolating the faulted line section. A DC fault could be isolated by tripping the AC CBs and the faulted line section could be isolated by opening DC disconnectors [2,3]. In addition to that, it was reported that the isolation of DC faults could also be achieved by the use of DC-DC converters [5,6], full-bridge/hybrid MMC [7–9] and hybrid DC CBs [10–14]. However, the technique of DC-DC converters is mainly limited due to the high losses and cost of DC-DC converters; the applications of full-bridge/hybrid MMCs are limited by increased losses and cost of switching devices compared with those of using the half-bridge MMCs; the hybrid DC CB has only been demonstrated on the voltage scale of laboratory, and may not be commercially available for real higher voltage applications, and the cost of such a DC CB is considerable.

Previous research predominantly focused on the control and protection at Phase 1 and Phase 2, while the control and protection strategy proposed so far has been rarely comprehensive for the system recovery/reconfiguration at Phase 3 after the fault isolation.

This paper investigates the control and protection process at Phase 2 and Phase 3 after the fault detection and mainly focuses on the control and protection sequence at Phase 3, of an OWF

* Corresponding author.
E-mail addresses: puyu.wang@hotmail.com (P. Wang), x.p.zhang@bham.ac.uk (X.-P. Zhang), paul.coventry@nationalgrid.com (P.F. Coventry), ray.zhang@nationalgrid.com (R. Zhang), lizhou1985@163.com (Z. Li).

http://dx.doi.org/10.1016/j.ijepes.2016.10.003
0142-0615/

Nomenclature

T_n	terminal n ($n = 1, \ldots, n$)	DFIG	doubly-fed induction generator
t_n	time n ($n = 1, \ldots, n$)	HVDC	high-voltage direct current
CB	circuit breaker	MTDC	multi-terminal HVDC
SM	sub-module	IGBT	insulated-gate bipolar transistor
VSC	voltage sourced converter	RTDS	real-time digital simulator
MMC	modular multilevel converter	AC CB	AC circuit breaker
OWF	offshore wind farm	DC CB	DC circuit breaker
OHL	overhead line		
PCC	point of common coupling		

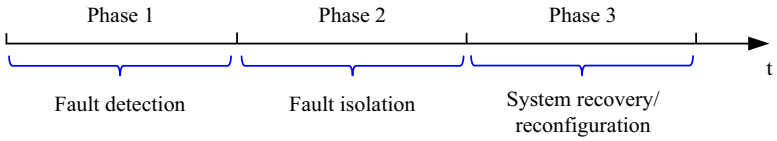

Fig. 1. Complete control and protection process against a fault.

integrated MMC MTDC system following DC faults. Since wind power has been recognized as one of the most promising renewables and its application is increasing at an annual rate of 20% [15,16], the integration of wind energy into electric power grids by HVDC technique, including the MTDC, has become particularly popular in recent years [15–17]. However, regarding the offshore integrated MTDC network, emphasis has been predominantly put on the grid integration of the OWFs [18,19], while less attention has been paid to the control and protection of the system following DC faults and the recovery/ reconfiguration control after the clearance/isolation of the fault.

Although the use of DC-DC converters, full-bridge/hybrid MMCs and hybrid DC CBs could become applicable in operation and may be more effective in dealing with DC faults in the future, it is necessary to comprehensively investigate a feasible control and protection strategy before they could become commercially available and viable.

In this paper, the control and protection strategy at the DC fault isolation phase is presented with detailed control and protection sequence, which would be useful for practical applications. Then the emphasis is put on the system recovery/reconfiguration sequence, including (1) when the recovery control should be started after the fault isolation; (2) the sequence between deblocking the MMCs and reclosing the AC CBs; and (3) the recovery sequence of each HVDC terminal. Based on the theoretical analysis, a preferred recovery/reconfiguration scheme is proposed. A 4-terminal MMC HVDC system with 1 terminal integrated with an OWF is established on the RTDS. The effectiveness of the proposed scheme is verified by real-time simulation results. The impact of transient and permanent DC faults at on the system recovery/reconfiguration control is discussed. In addition, the recovery/reconfiguration control of the MTDC in radial and meshed topologies is compared and demonstrated. Synthesizing the analytical and simulation studies, a general guideline for the recovery/reconfiguration control of MMC MTDC systems is proposed.

The rest of this paper is organized as follows. Section 2 presents the system configuration, the basic control modes of the MMCs and the DFIG-based OWF, and the system fault isolation strategy. The system recovery/reconfiguration control and protection sequence is comprehensively investigated and a preferred scheme is proposed in Section 3. Case studies are demonstrated in Section 4. A general guideline on the recovery/reconfiguration control of MMC MTDC systems is proposed in Section 5. Several conclusions are drawn in Section 6.

2. Offshore integrated MMC MTDC system

This section presents the investigated system configuration, control modes of the MMCs and the DFIG, and the system DC fault isolation strategy.

2.1. System configuration

Fig. 2 shows a single-line schematic diagram of a 4-terminal MMC HVDC system with the integration of an OWF. T_n ($n = 1, \ldots, 4$) denotes each terminal of the MTDC system. MMC-n ($n = 1, \ldots, 4$) denotes the MMC at each terminal. On the AC side of the MTDC system, the OWF is connected with T_1 of the MTDC system. The OWF consists of 60 wind turbines. *CBW* denotes the AC CB of the wind farm. *CBn* ($n = 2, \ldots, 4$) denotes the AC CB at each terminal. On the DC side, DC *ISWn* ($n = 1, \ldots, 4$) denotes the DC isolation switch and is equipped at each terminal. The DC grid is modeled by DC OHL. The length of each DC OHL is 100 km. The MMC at each terminal is half-bridge, 7-level converter. Fig. 3 illustrates the structure of MMC-n. The system parameters at each terminal are the same, only the control modes of the MMCs are different. Detailed parameters of the system are shown in Table 1.

2.2. Basic control mode

The control mode of the MMC at each HVDC terminal and the DFIG is briefly introduced as follows.

2.2.1. MMCs

Since the OWF is integrated at T_1, AC voltage and frequency (V_{ac}-f) control [18] is employed by MMC-1 to stabilize the magnitude and frequency of the AC voltage at the PCC for the integration of the OWF. The other three MMCs apply the well-known dq decoupled control. Regarding the power balancing in the MTDC systems, two main control paradigms, master-slave control [20–22] and voltage droop control [23–25], are generally utilized. In the following analysis, master-slave control is applied for the MTDC: MMC-2 is operated as the master terminal controlling the DC voltage; MMC-3 and MMC-4 are both operated as power dis-

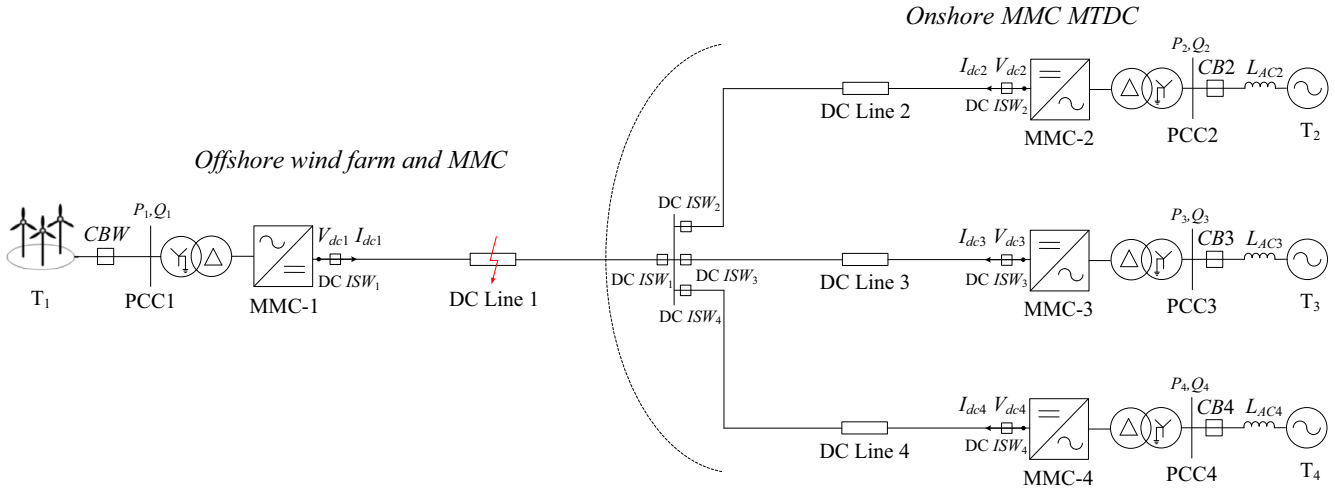

Fig. 2. Configuration of the offshore integrated 4-T MMC HVDC system.

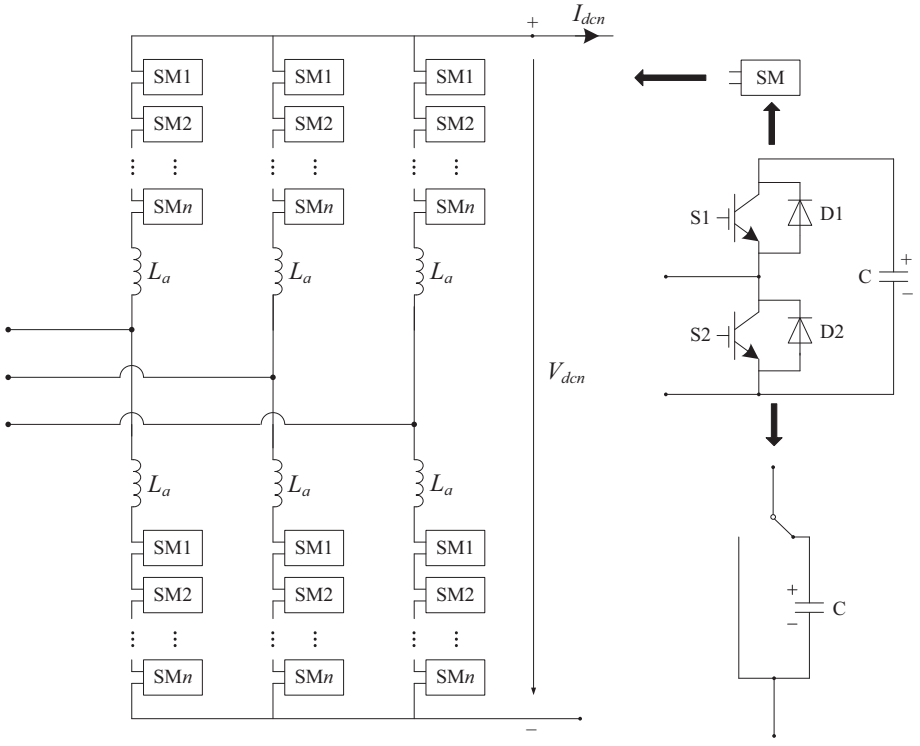

Fig. 3. Structure of MMC-*n*.

Table 1
Parameters of the offshore integrated 4-T MMC VSC HVDC system.

Description	Value
MMC rated capacity	150 MVA
Nominal AC voltage	138 kV
L_{AC}	150 mH
Transformer voltage ratio	138 kV/30 kV (Y/Δ)
Transformer rating	150 MVA
Transformer leakage inductance	5%
Nominal DC voltage	±50 kV
SM capacitance	1500 μF
Wind farm rated output	84 MW
Length of DC line n	100 km

patchers where 50 MW is imported into the DC grid from T_3, while 90 MW is exported to T_4 from the DC grid. The control and protection sequence of the MTDC with droop control will also be discussed.

The capacitor balancing strategy with the conventional sorting method [26] is applied by the MMCs. That is the SMs with lower capacitor voltages are charged first, while the SMs with higher capacitor voltages are discharged first depending on the direction of the arm current. The number of SMs being charged/discharged is generated from the converter reference signals, which have been committed to implement either V_{ac}-f control or dq decoupled control based on their control modes.

2.2.2. DFIG

The DFIG is modeled based on [27,28]. Both the grid VSC and rotor VSC employ *dq* decoupled control. The grid VSC regulates the DC capacitor voltage of the back-to-back converter and reactive power. The rotor VSC controls electrical torque and rotor excitation current.

2.3. DC fault isolation strategy

For the symmetrical monopole configuration, pole-to-pole DC fault is considered to be more critical than a pole-to-ground fault [29]. This is because the latter one will not bring any overcurrent and will only result in overvoltage on the unfaulted pole [30], which can be de-energized by switching on a solid-state switch with a discharging resistor as a DC chopper. However, the former one will result in remarked overcurrents, which may damage the system components. Such a critical condition necessitates immediate control and protection actions, which are the main focus of this paper.

When a pole-to-pole DC fault occurs, the blocking of MMCs is required to be swiftly implemented to protect the IGBTs [1–3]. The delay of the blocking action following the fault has significant impact on the power electronic devices and the DC line. In this paper, it is assumed that the blocking action of MMCs is activated if the DC currents increase over 1.2 p.u. of its nominal value [31–32], which is the assumed current threshold. After blocking the MMCs, the MMCs become uncontrolled diode bridges and their operating condition can be simplified as shown in Fig. 4.

Due to the unilateral conductive characteristic of diode, AC networks can still inject power into the DC side through the MMCs. Therefore, in an MTDC grid without the installation of DC CBs or DC-DC converters, the isolation of a DC fault is by tripping all the AC CBs at the adjacent HVDC terminals. The fault will be isolated after tripping all AC CBs and the DC currents will gradually decay. DC ISW_1 will be opened when the DC current at T_1 becomes sufficiently small to isolate the faulted line.

A pole-to-pole fault on DC Line 1 as shown in Fig. 2 is simulated on the RTDS. The control and protection sequence at the fault isolation phase is depicted in Fig. 5 and the time delay between 2 sequential control actions is shown Table 2. According to practical applications, the AC CBs can be tripped within 60–100 ms. In the case study, it is assumed that the AC CBs are tripped with 80 ms and DC ISW_1 will be opened at current-passing-zero point. In the case studies, V_{dcn} $(n = 1, \ldots, 4)$ represents the DC voltage at T_n, respectively. I_{dcn} $(n = 1, \ldots, 4)$ represents the DC current at T_n, respectively. P_n and Q_n $(n = 1, \ldots, 4)$ represent the active power and reactive power at T_n, respectively. The measuring points of the quantities are illustrated in Figs. 2 and 3.

The simulation results are shown in Fig. 6 where (a) shows the DC voltages of the MTDC; (b) shows the DC currents of the MTDC; and (c) shows the zoomed proportion after the fault occurs of (b).

Due to the pole-to-pole fault, the DC voltages of the MTDC drop close to zero as shown in Fig. 6(a). Fig. 6(c) shows that the DC current at T_1 increases significantly and surpasses the current threshold 1.2 p.u. within 2 ms, which activates the blocking of the MMCs. The fault is isolated when all the AC CBs are tripped. Fig. 6(b) shows that the DC currents decrease to zero without feeding into the faulted point, which indicates the effectiveness of the fault isolation strategy. The faulted line section is isolated when DC ISW_1 is opened at current-crossing-zero point at 5.6 s

3. Control and protection sequence for recovery/ reconfiguration after fault isolation

A fault on a DC OHL can be either transient or a permanent. This paper takes both transient and permanent DC faults into account, especially the control and protection sequence after the fault isolation phase. This is because a transient fault can be cleared after the fault isolation and with appropriate recovery control, the MTDC

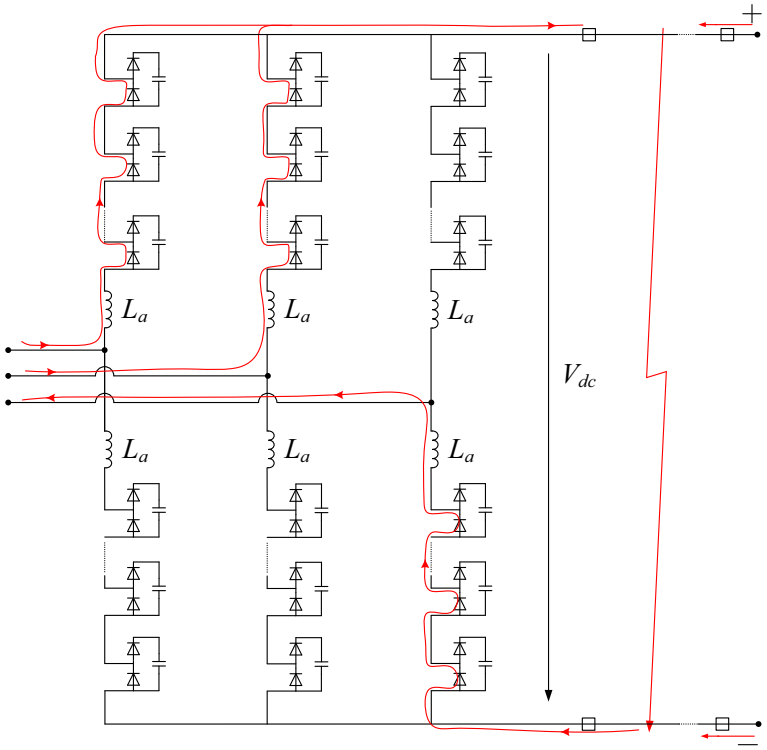

Fig. 4. System operating condition after blocking the MMCs.

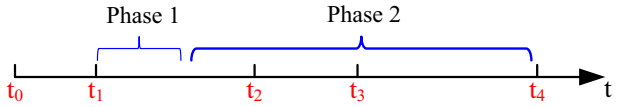

Fig. 5. Control and protection sequence of the DC fault isolation.

Table 2
Description of the action of the control and protection sequence in Fig. 5.

t_n	Time (s)	Description
t_0	0	MTDC under normal operation
t_1	4	Fault applied on DC Line 1
t_2	4.002	All MMCs blocked
t_3	4.08	All AC *CBs* tripped and OWF blocked
t_4	5.6	DC ISW_1 opened

system can resume original operating condition. However, after the isolation of a permanent fault, the faulted terminal cannot resume, the MTDC system will be reconfigured with the recovery of the unfaulted terminals.

It is vital to consider the following 3 issues during the system recovery phase.

(a) At what time is it appropriate to start the recovery/reconfiguration control after the fault isolation?

(b) Which action should be conducted first, deblocking of the MMCs or reclosing of the AC CBs?

(c) Which HVDC terminal should resume first to operate and which sequence is the best for the performance of the recovery/reconfiguration of the MTDC system?

The above issues will be discussed and analyzed in the following sections and the MTDC system under a transient DC fault will be taken as an example. The situation under a permanent DC fault will be analyzed afterwards.

3.1. When to start the recovery control

For an MTDC system after the fault isolation, the system condition is that all the MMCs are blocked and all the AC CBs are open. The faulted line section is isolated at 5.6 s by opening DC ISW_1 when the DC current of T_1 decays to zero. At that moment, the DC currents of the other three HVDC terminals are still decreasing and have not completely decayed to zero. There may be oscillations if the recovery/reconfiguration control is started immediately after opening of DC ISW_1. Hence, the recovery/reconfiguration control in this paper is started when all the DC currents have completely decayed to zero.

3.2. Sequence between deblocking of MMCs and reclosing of AC CBs

For T_1, since the integration of the OWF needs to be implemented with the stabilization of the voltage at PCC1, which neces-

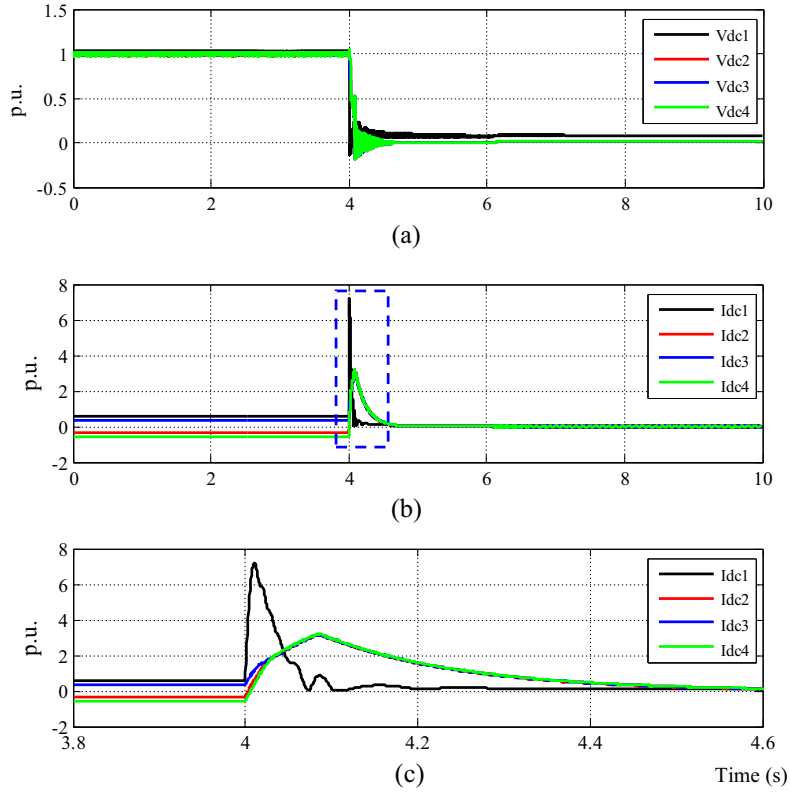

Fig. 6. Characteristics of MMC-1 DC side current with DC fault isolation.

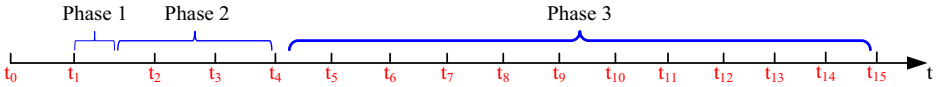

Fig. 7. Complete control and protection sequence for the radial MTDC system under a transient DC fault on DC Line 1.

Table 3
Description of the action of the control and protection sequence in Fig. 7.

t_n	Time (s)	Description
t_0	0	MTDC under normal operation
t_1	4	Fault applied on DC Line 1
t_2	4.002	All MMCs blocked
t_3	4.08	All AC *CBs* tripped and OWF blocked
t_4	5.6	DC ISW_1 opened, fault cleared
t_5	7	T_1 DC ISW_1 reclosed
t_6	7.5	*CB*2 reclosed
t_7	8.0	MMC-2 deblocked
t_8	8.5	*CB*3 reclosed
t_9	9	Set $P_{3ref} = 0$, MMC-3 deblocked
t_{10}	9.5	*CB*4 reclosed
t_{11}	10.0	Set $P_{4ref} = 0$, MMC-4 deblocked
t_{12}	10.5	MMC-1 deblocked
t_{13}	16.5	CBW reclosed
t_{14}	17.5	OWF deblocked
t_{15}	25.0	Ramp P_{4ref}, P_{3ref} to the nominal values

sitates the inverted control of the DC-side voltage of MMC-1. Hence, *CBW* will be reclosed after the deblocking of MMC-1.

For the other 3 terminals with AC voltage sources, one sequence is to deblock the MMCs first, followed by reclosing the AC CBs. In this way, the arm current of the MMC will flow through the IGBTs after reclosing the AC CBs. The IGBTs may be damaged if there are large inrush currents. However, with the contrast approach, the reclosing of AC CBs is implemented prior to the deblocking of MMCs; there will be no current flowing through IGBTs, since all MMCs are still blocked and the SM capacitors are in energization mode [33] at this stage, which thereby reduces the voltage spikes and current surges when deblocking the MMCs.

Therefore, for T_1, MMC-1 will be deblocked prior to the reclosing of CB1, while for the other 3 terminals, AC CBs will be reclosed prior to the deblocking of the MMCs.

3.3. Recovery sequence of each HVDC terminal

Due to different control modes of the MMCs at each HVDC terminal, the recovery sequence of each terminal has large impacts on the performance of the system recovery. MMC-1 applies V_{ac}-f control, necessitating a stable voltage at the MMC DC side, to stabilize the voltage at PCC1 for the integration of the OWF. Hence, T_2 should resume prior to that of T_1 to establish the DC grid voltage. In addition, Due to the fact that T_1 is connected with the wind farm, the AC network of T_1 is regarded as a weaker network with respect

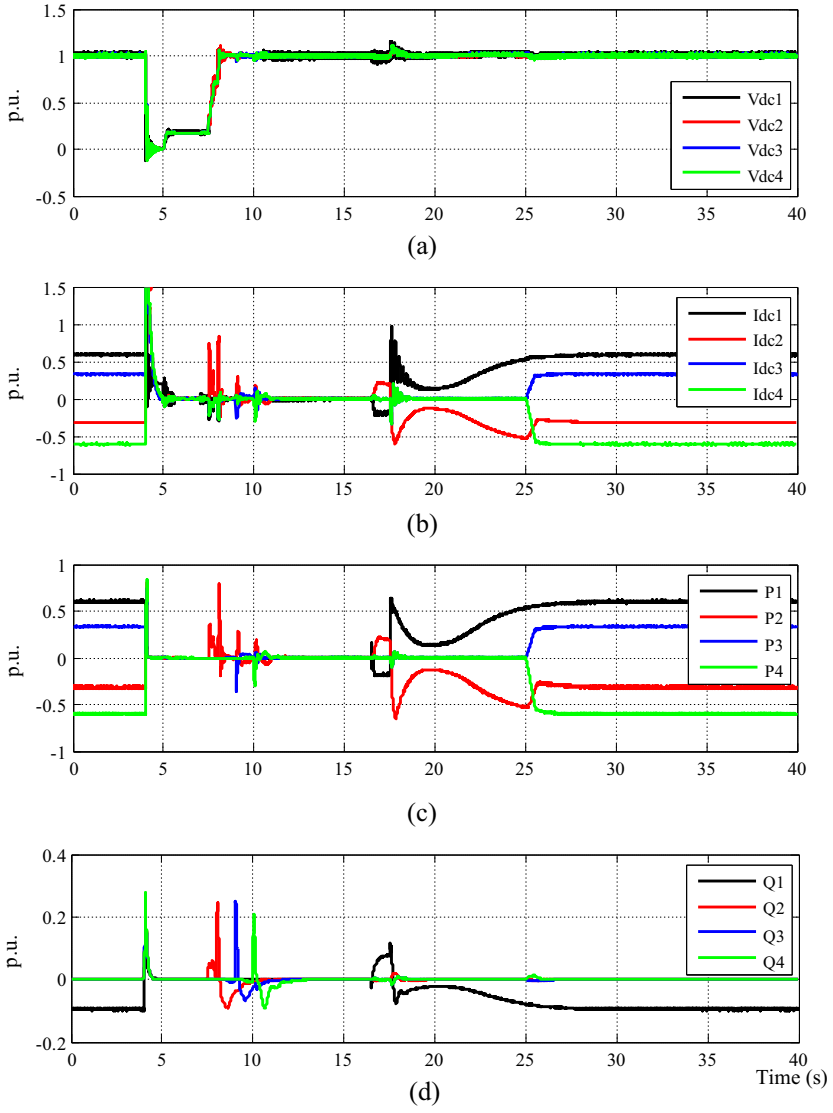

Fig. 8. System performance under a transient DC fault on DC Line 1 with the proposed control and protection sequence: (a) DC voltages of the MTDC, (b) DC currents of the MTDC, (c) active power, and (d) reactive power.

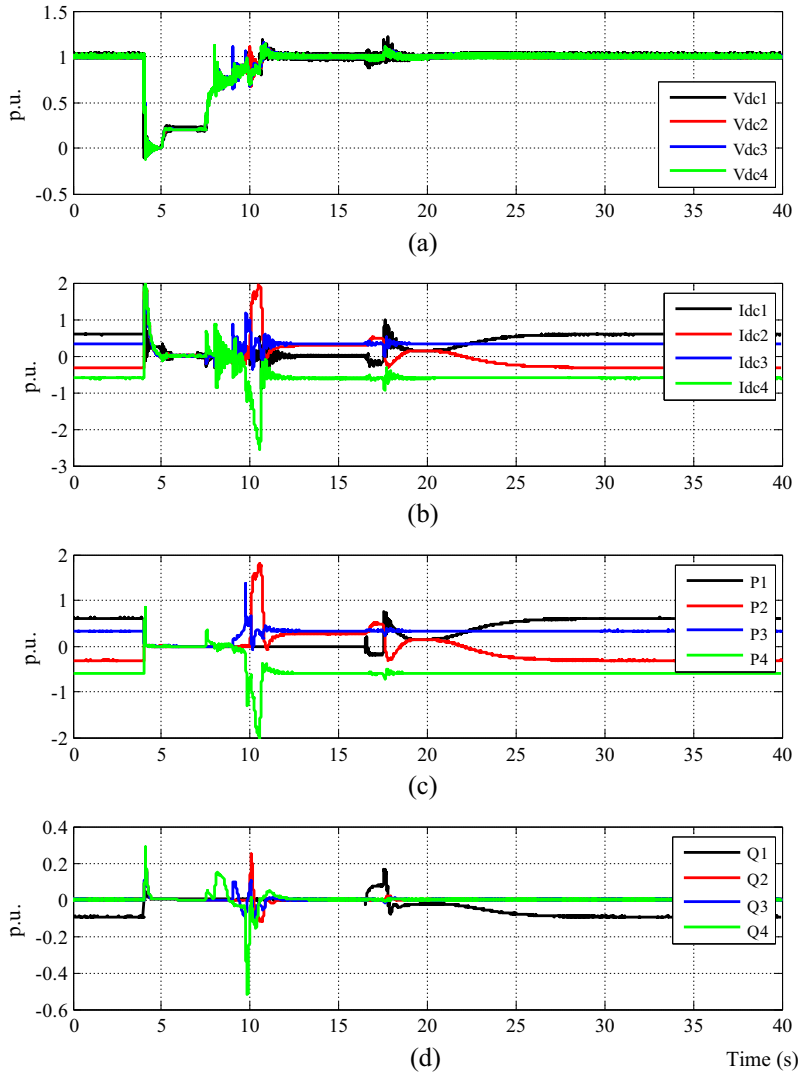

Fig. 9. System performance under a transient DC fault on DC Line 1 with a different recovery sequence: (a) DC voltages of the MTDC, (b) DC currents of the MTDC, (c) active power, and (d) reactive power.

to those of the other three terminals. Therefore, it would be beneficial to resume T_1 after the resume of the other terminals, the process of which will not be affected by T_1, such as the wind intermittency. As the master terminal, T_2 stabilizes the DC voltage, which acts as a DC slack bus. It would be beneficial to firstly resume MMC-2 for the re-establishment of the DC grid voltage and then to resume the remaining terminals. Due to the fact that T_3 and T_4 are both operated as power dispatchers, the active power references of both terminals will be set to zero after deblocking, so that the master terminal does not need to compensate the loss of power of T_1 during the recovery of both terminals. The active power references of both terminals will ramp to the nominal values when the recovery of T_1 has been completed and the OWF imports stable power into the DC grid. Hence, the recovery sequence of each HVDC terminal is T_2, T_3, T_4, T_1.

In terms of a permanent DC fault, the faulted terminal will not resume, while the recovery sequence of the other terminals is the same as that of the transient fault and is considered as a reconfiguration sequence.

4. Case studies

5 case studies are conducted on the RTDS.

- *In Case A, the performance of the investigated system under a transient DC fault using the proposed recovery/reconfiguration sequence is demonstrated.*
- *Case B is similar to Case A, except that a different recovery/reconfiguration control sequence is applied so as to compare the system performance with that in Case A.*
- *In Case C, the system performance under a permanent DC fault with the proposed reconfiguration sequence is presented.*
- *Case D is similar to Case C, except that the MTDC uses droop control instead of master-slave control. Since the voltage droop control has been mainly used on the MTDC, the objective of Case D is to evaluate the proposed recovery/reconfiguration sequence on the MTDC with droop control.*
- *Case E is similar to Case C, except that the MTDC is in meshed topology instead of radial topology. Since the MTDC grid can be in either radial or meshed topology, the objective of Case E is to evaluate the proposed recovery/reconfiguration sequence on the meshed MTDC.*

4.1. Transient DC fault with the proposed recovery control

In this case, a transient pole-to-pole fault at T_1 is applied at 4 s on DC Line 1. The fault isolation is conducted as that proposed in Section 2. The transient fault is cleared when DC arc at the faulted

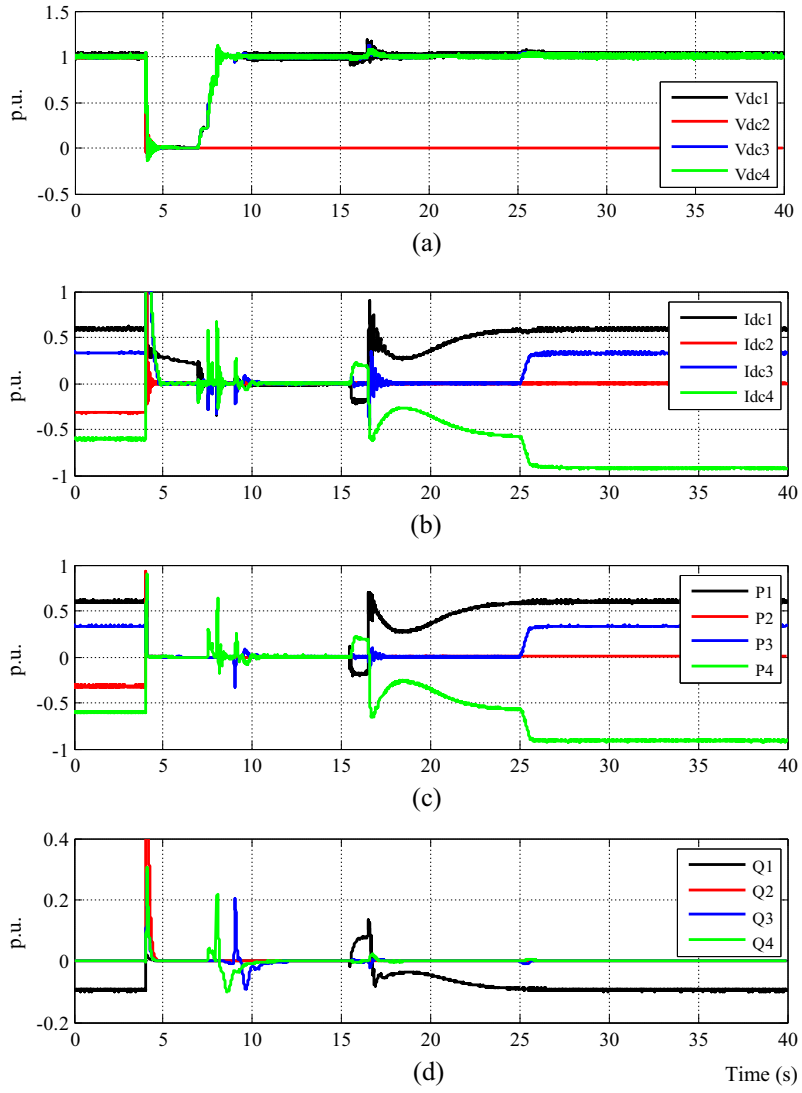

Fig. 10. System performance under a permanent DC fault on DC Line 2 with the proposed control and protection sequence: (a) DC voltages of the MTDC, (b) DC currents of the MTDC, (c) active power, and (d) reactive power.

point has been extinguished. Generally, DC arc can be extinguished when the current becomes sufficiently small [34,35]. The current on DC Line 1 completely decays to zero after opening DC ISW_1 and the fault is assumed to be cleared at that time.

As discussed in Section 3, the recovery control is initiated with reclosing DC ISW_1 when the currents on the MTDC grid have completely decayed to zero. The following recovery sequence is the same as proposed in Section 3. The overall control and protection sequence is shown in Fig. 7 with descriptions in Table 3. The delay between 2 sequential control actions, i.e. the control actions at t_k and t_{k+1} ($k = 1, \ldots, 14$).

The system performance is shown in Fig. 8, where (a) shows the DC voltages of the MTDC, (b) shows the DC currents of the MTDC, (c) shows the active power, and (d) shows the reactive power.

The system performance at the fault isolation phase has been discussed in Section 2. Here, we only look at the performance at the system recovery phase. The recovery control is initiated with reclosing DC ISW_1 at 7 s. Fig. 8(a) demonstrates that the DC voltages of the MTDC resume the nominal condition after reclosing *CB*2 and deblocking MMC-2. Fig. 8(b) shows that DC currents resume in sequence to nominal operating condition with small current surges, which are less than 1 p.u. Fig. 8(c) shows that the active power of each terminal is well controlled and the OWF is successfully re-integrated and exporting power to the grid. In Fig. 8(d), oscillations of the reactive power are less than 0.3 p.u. The simulation results shown in Fig. 8 demonstrate that the proposed control and protection scheme is effective under the transient DC fault condition and the MTDC resumes in a stable and smooth manner.

4.2. Transient DC fault with a different recovery control

In this case, the fault applied and the fault isolation strategy are the same as those of *Case A*. However, during the recovery phase, the deblocking sequence of the MMCs applied is different. The differences are: (1) recovery sequence is T_4, T_3, T_2, T_1 instead of T_2, T_3, T_4, T_1; (2) the active power references of MMC-3 and MMC-4 are kept at nominal values. The system performance is shown in Fig. 9, where (a) shows the DC voltages of the MTDC, (b) shows the DC currents of the MTDC, (c) shows the active power, and (d) shows the reactive power.

Fig. 9(a) demonstrates that the DC voltages of the MTDC do not reach the nominal operating condition until the recovery of MMC-2 and the voltage oscillations are more significant in comparison

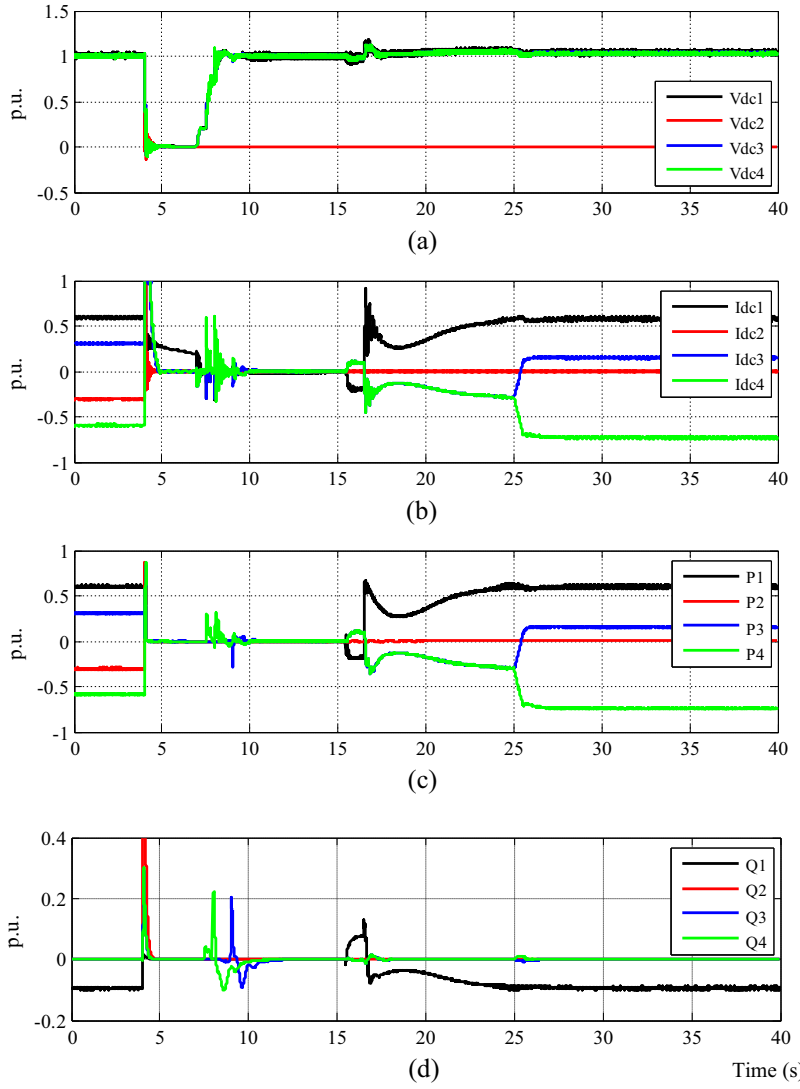

Fig. 11. System performance with droop control under a permanent DC fault on DC Line 2 with proposed control and protection sequence: (a) DC voltages of the MTDC, (b) DC currents of the MTDC, (c) active power, and (d) reactive power.

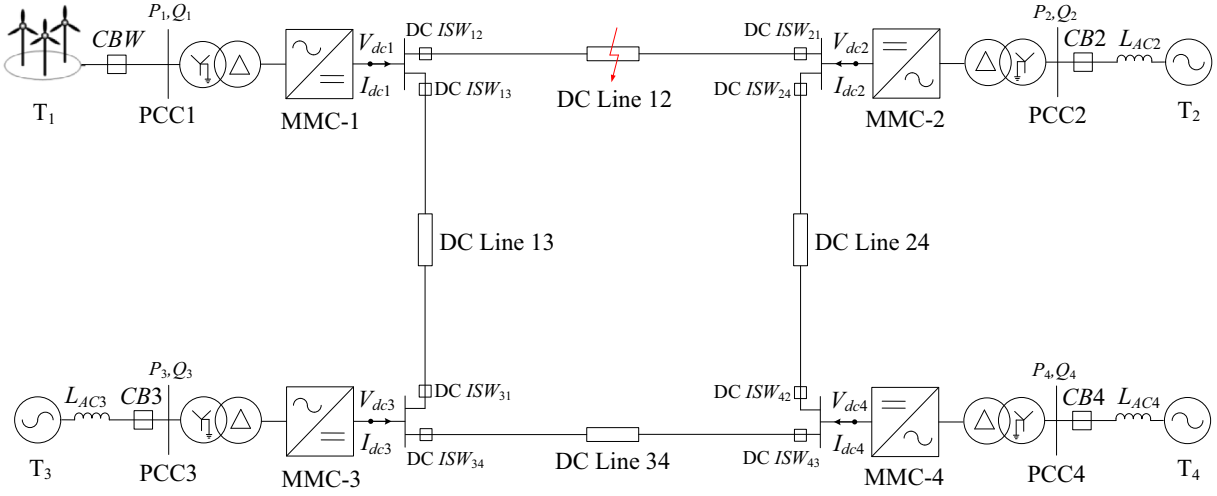

Fig. 12. Configuration of the offshore integrated 4-T MMC HVDC system in meshed topology.

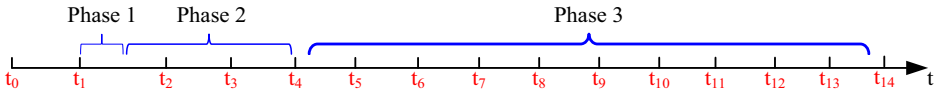

Fig. 13. Complete control and protection sequence for the meshed MTDC system under a permanent DC fault on DC Line 12.

Table 4
Description of the action of the control and protection sequence in Fig. 13.

t_n	Time (s)	Description
t_0	0	MTDC under normal operation
t_1	4	Fault applied on DC Line 12
t_2	4.002	All MMCs blocked
t_3	4.08	All AC *CBs* tripped and OWF blocked
t_4	5.6	DC ISW_{12} and DC ISW_{21} opened, permanent fault isolated
t_5	7.5	*CB*2 reclosed
t_6	8.0	MMC-2 deblocked
t_7	8.5	*CB*3 reclosed
t_8	9	Set $P_{3ref} = 0$, MMC-3 deblocked
t_9	9.5	*CB*4 reclosed
t_{10}	10.0	Set $P_{4ref} = 0$, MMC-4 deblocked
t_{11}	10.5	MMC-1 deblocked
t_{12}	16.5	CBW reclosed
t_{13}	17.5	OWF deblocked
t_{14}	25.0	Ramp P_{4ref}, P_{3ref} to the nominal values

with those in Fig. 8(a). Fig. 9(b) shows that the DC currents at T_2 and T_4 exceed the current threshold at 10 s after deblocking MMC-2. In Fig. 9(c), significant oscillations of active power can be observed after deblocking MMC-2. The oscillations at T_4 reach a peak of 2 p.u. Simulation results show that more oscillations emerge at the system recovery phase using the different recovery sequence. Therefore, the recovery control sequence proposed in *Case A* is regarded to be more appropriate for the system recovery after the clearance of a transient fault. For transient DC faults occurring at the other terminals, the proposed scheme can be similarly applied.

4.3. Permanent DC fault

Different with the previous cases, the fault applied in this case is a permanent DC fault. If the permanent fault occurs at one of the slave terminals, similar recovery sequence can be applied after the fault isolation and the MTDC system will be reconfigured into a 3-terminal system. However, if the permanent fault occurs at the master terminal, the system recovery control will become more complex. In this case, the permanent DC fault is assumed to occur on DC Line 2. Due to a permanent fault, T_2 will not resume after the fault isolation. If the unfaulted terminals are scheduled to resume operation, one of the terminals, T_3 or T_4, needs to switch control mode to take over the DC voltage control. After that, similar recovery sequence can be applied to resume the unfaulted terminals. In this case, T_4 is selected to switch control mode to maintain the DC voltage after the fault isolation. The system performance is shown in Fig. 10, where (a) shows the DC voltages of the MTDC, (b) shows the DC currents of the MTDC, (c) shows the active power, and (d) shows the reactive power.

Fig. 10(a) demonstrates that T_4 takes over the DC voltage control after the fault isolation and the DC voltage is well maintained after the recovery of T_4. Fig. 10(b) shows that the DC currents of the MTDC resume in sequence with small current surges. The active power of the unfaulted terminals is well controlled and resumes smoothly in sequence as shown in Fig. 10(c). Hence, the simulation results prove the effectiveness of the reconfiguration control after the permanent fault at the master terminal. However, in real applications, it is generally not desired to switch the control mode of one converter during operation [20,35]. Another solution for the system reconfiguration control, which can avoid the switching of control mode of one MMC, is to let the MTDC apply voltage droop control instead of the master-slave control.

4.4. MTDC with droop control

In this case, the MTDC system applies voltage droop control. Since the DC voltage control can be shared among different converters with voltage droop control, the MTDC can resume without switching control mode of any terminal regardless the location of a permanent fault. In this case, T_2, T_3, and T_4 apply coordinated droop control and the same permanent fault is applied on DC Line 2. The system performance is shown in Fig. 11, where (a) shows the DC voltages of the MTDC, (b) shows the DC currents of the MTDC, (c) shows the active power, and (d) shows the reactive power.

Due to the application of voltage droop control, the voltage support of the MTDC grid can be shared by T_3 and T_4 after the fault isolation. Fig. 11(a) demonstrates that the nominal DC voltage is established without switching control mode of any MMC. Fig. 11 (b) shows that the DC currents of the MTDC resume smoothly with small current surges. The active power is shared among T_3 and T_4 as shown in Fig. 11(c). However, in *Case C*, after taking over the DC voltage control, T_4 operates as a slack terminal to balance the power exported from T_1 and T_3, which leads to the phenomenon that the active power transferred at T_4 is close to 1 p.u. as shown in Fig. 10(c). Since the system recovery after the fault isolation does not necessitate switching the control mode of any terminal, the system recovery control becomes easier and more efficient. This case also indicates that the control and protection sequence proposed can be applied for the MTDC with droop control.

4.5. MTDC in a meshed topology

In this case, the MTDC is connected in meshed topology as illustrated in Fig. 12.

When a permanent DC fault occurs on DC Line 12, the control and protection approach at the phase of fault isolation and faulted section isolation is the same as that in the previous cases. After the isolation of the faulted line section, all the MMCs and the remaining three unfaulted DC lines can resume operation due to the fact that the MTDC is in meshed configuration. The overall control and protection sequence is shown in Fig. 13 with descriptions in Table 4. The delay between 2 sequential control actions, i.e. the control actions at t_k and t_{k+1} ($k = 1, \ldots, 13$).

The performance of the meshed 4-terminal MMC HVDC system is shown in Fig. 14, where (a) shows the DC voltages of the MTDC, (b) shows the DC currents of the MTDC, (c) shows the active power, and (d) shows the reactive power.

Fig. 14(a) demonstrates that the DC voltages are well established after the isolation of the faulted line section. Fig. 14(b) demonstrates that all the MMCs and the remaining three unfaulted DC lines resume operation after the faulted section isolation due to the meshed MTDC topology. In addition, the adjacent four AC networks resume importing/exporting power as shown in Fig. 14(c). However, in *Case C* and *Case D*, the faulted MMC-2 cannot resume after the fault isolation as shown in Figs. 10 and 11 due to the radial topology of the MTDC. Hence, the comparison case studies also demonstrate the higher flexibility of meshed MTDC over the radial MTDC.

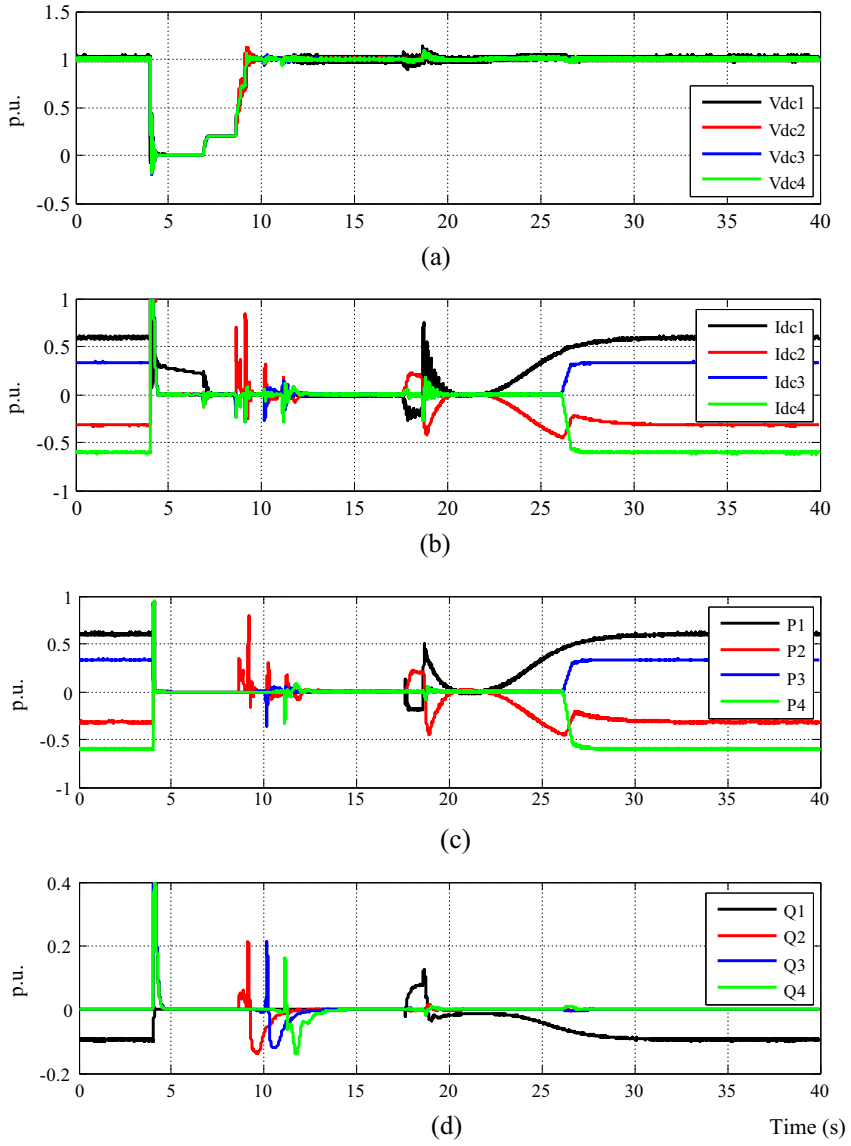

Fig. 14. Performance of the meshed MTDC system under a permanent DC fault on DC Line 12 with the proposed control and protection sequence: (a) DC voltages of the MTDC, (b) DC currents of the MTDC, (c) active power, and (d) reactive power.

5. General guideline for the system recovery/reconfiguration control

Based on the analysis in Section 3 and the case studies in Section 4, a general guideline on the system recovery/reconfiguration control is proposed for MMC MTDC systems after the phase of fault isolation.

For an MMC MTDC system, the terminals can be divided into 2 types of terminals, namely Terminal A and Terminal B: For Terminal A, the voltage at the PCC can be well stabilized by the AC network; For Terminal B, the stabilization of the voltage at the PCC necessitates the inverted control of the MMC.

- The system recovery control will start when the DC currents on the DC grid have completely decayed to zero.
- Terminal A will resume prior to the resume of Terminal B.
  - For Terminal A,
    the AC CBs will be reclosed prior to the deblocking of the MMCs;
    if there is no terminal with DC voltage control or voltage droop control, one terminal need to switch control mode to take over the DC voltage control;
    the terminals with DC voltage control or voltage droop control will resume prior to the resume of the terminals with active power control.
  - For Terminal B,
    the MMCs will be deblocked prior to the reclosing of the AC CBs.
- For 2 sequential control actions, the latter action should be conducted when the system reaches a new stable condition after the former action.
- The reference setting of each terminal should be appropriately adjusted to optimize the system performance.

6. Conclusion

This paper has investigated the control and protection sequence of an offshore integrated MMC MTDC system with two control

paradigms, master-slave control and voltage droop control, under DC fault conditions. The fault isolation with detailed control and protection sequence has been presented. The system recovery/reconfiguration control after the fault clearance/isolation has been comprehensively analyzed regarding (1) the time of starting the system recovery control, (2) control sequence between the deblocking of MMCs and reclosing of AC CBs, and (3) recovery sequence of each HVDC terminal. A preferred recovery/reconfiguration scheme has been proposed based on the analysis of the system characteristics and validated by the simulation results on the RTDS. The impact of transient and permanent DC faults on the MTDC system has been discussed. For a transient DC fault occurring at one of the slave terminals, system performance using different recovery control sequences has been compared and the proposed recovery sequence has demonstrated its superiority for the system recovery with fewer voltage spikes and current surges. For a permanent DC fault occurring at the terminal with DC voltage control, the reconfiguration control has been compared between the MTDC with master-slave control and voltage droop control. The MTDC with droop control can resume the unfaulted terminals more efficiently without switching control mode of any terminal and can share the active power among the HVDC terminals. Furthermore, the performance of the recovery/reconfiguration control of the MTDC in radial and meshed topologies has been compared and demonstrated. Synthesizing the analysis and simulation case studies, a general guideline for the recovery/reconfiguration control of MMC MTDC systems has been proposed. The proposed control and protection sequence approach would be widely applicable for VSC based MTDC grids.

Acknowledgements

This work was supported in part by EPSRC under Grant EP/K006312/1, National Grid, U.K., and the School of EESE, University of Birmingham.

References

[1] Zhang X-P, Zhang R, Coventry PF. Fault management of the MT VSC HVDC using Delayed Auto-Re-Configuration (DARC) schemes. Project Report for National Grid; 2011.
[2] Wang P, Li Z, Zhang X-P, Zhang R, Coventry PF. DC fault management for VSC MTDC system using delayed-auto-re-configuration scheme. In: 11th IET international conference on AC DC power transmission, Birmingham, UK. p. 1–7.
[3] Tang L, Ooi B-T. Locating and isolating DC faults in multiterminal DC systems. IEEE Trans Power Deliv 2007;22(3):1877–84.
[4] Kerf KD, Srivastava K, Reza M, Bekaert D, Cole S, Hertem DV, Belmans R. Wavelet-based protection strategy for DC faults in multi-terminal VSC HVDC systems. IET Gen Transm Distrib 2011;5(4):496–503.
[5] Jovcic D, Ooi B-T. Developing DC transmission networks using DC transformers. IEEE Trans Power Deliv 2010;25(4):2535–43.
[6] Kish G, Ranjram M, Lehn P. A modular multilevel DC/DC converter with fault blocking capability for HVDC interconnects. IEEE Trans Power Electron 2015;30(1):148–62.
[7] Marquardt R. Modular multilevel converter topologies with dc-short circuit current limitation. In: Proceedings of the IEEE 8th international power electronics ECCE Asia conference. p. 1425–31.
[8] Merlin M, Green TC, Mitcheson P, Trainer DR, Critchley R, Crookes W, Hassan F. The alternate arm converter: a new hybrid multilevel converter with dc-fault blocking capability. IEEE Trans Power Deliv 2014;29(1):310–7.
[9] Feldman R, Farr E, Watson AJ, Clare JC, Wheeler PW, Trainer DR, Crookes RW. DC fault ride-through capability and STATCOM operation of a HVDC hybrid voltage source converter. IET Gen Transm Distrib 2014;8(1):114–20.
[10] Callavik M, Blomberg A, Häfner J, Jacobson B. The hybrid HVDC breaker. ABB grid systems Technical Paper, November 2012.
[11] Franck CM. HVDC circuit breakers: a review identifying future research needs. IEEE Trans Power Deliv 2011;26(2):998–1007.
[12] Bucher MK, Franck CM. Contribution of fault current sources in multiterminal HVDC cable networks. IEEE Trans Power Deliv 2013;28(3):1796–803.
[13] Hadjikypris M, Terzija V. Transient fault studies in a multi-terminal VSC-HVDC grid utilizing protection means through DC circuit breakers. In: IEEE PowerTech, Grenoble, France. p. 1–6.
[14] Kontos E, Pinto RT, Rodrigues S, Bauer P. Impact of HVDC transmission system topology on multiterminal DC network faults. IEEE Trans Power Deliv 2015;30(2):844–52.
[15] Bellmunt O, Alvarez A, Ferre A, Liang J, Ekanayake J, Jenkins N. Multiterminal HVDC-VSC for offshore wind power integration. In: IEEE power and energy society general meeting. p. 1–6.
[16] Forster H, Healy S, Loreck C, Matthes F. Analysis of the EU's energy roadmap 2050 scenarios. Smart energy for Europe platform; 2012.
[17] Chen X, Sun H, Wen J, Lee W-J, Yuan X, Li N, Yao L. Integrating wind farm to the grid using hybrid multiterminal HVDC technology. IEEE Trans Indust Appl 2011;47(2):965–72.
[18] Kirby NM, Xu L, Luckett M, Siepmann W. HVDC transmission for large offshore wind farms. IEE Power Eng J 2002;16(3):135–41.
[19] Gnanarathna UN, Chaudhary SK, Gole AM, Teodorescu R. Modular multi-level converter based HVDC system for grid connection of offshore wind power plant. In: 9th IET international conference on AC DC power transmission, London, UK. p. 1–5.
[20] Haileselassie TM. Control, dynamics and operation of multi-terminal VSC-HVDC transmission systems [Ph.D. dissertation]. Trondheim (Norway): Norwegian University of Science and Technology; 2012.
[21] Cao J, Du W, Wang HF, Bu SQ. Minimization of transmission loss in meshed AC/DC grids with VSC-MTDC networks. IEEE Trans Power Syst 2013;28(3):3047–55.
[22] Yousefpoor N, Kim S, Bhattacharya S. Multi-terminal DC grid control under loss of terminal station. In: IEEE energy conversion congress and exposition (ECCE). p. 744–9.
[23] Haileselassie TM, Uhlen K. Power system security in a meshed North Sea HVDC grid. Proc IEEE 2013;101(4):978–90.
[24] Dierckxsens C, Srivastava K, Reza M, Cole S, Beerten J, Belmans R. A distributed DC voltage control method for VSC MTDC systems. Elect Power Syst Res 2012;82(1):54–8.
[25] Wang W, Barnes M. Power flow algorithms for multi-terminal VSC-HVDC with droop control. IEEE Trans Power Syst 2014;29(4):1721–30.
[26] Saeedifard M, Iravani R. Dynamic performance of a modular multilevel back-to-back HVDC system. IEEE Trans Power Deliv 2010;25(4):2903–12.
[27] Pena R, Clare JC, Asher GM. Doubly fed induction generator using back-to-back PWM converters and its application to variable-speed wind-energy generation. Proc Inst Elect Eng 1996;143(3):231–41.
[28] RTDS user's document. Wind-turbine driven doubly-fed induction generator. RTDS Technologies Inc.; 2011.
[29] International Electrotechnical Commission. High-voltage direct current (HVDC) transmission using voltage sourced converters (VSC). IEC Tech Rep IEC/TR 62543; 2011.
[30] Woodford D. Symmetrical monopole VSC transmission. Electranix Technical Paper, March 2014.
[31] Merlin MMC, Green TC, Mitcheson P, Trainer D, Critchley R, Crookes W, Hassan F. The alternate arm converter: a new hybrid multilevel converter with DC-fault blocking capability. IEEE Trans Power Deliv 2014;29(1):310–7.
[32] Judge PD, Merlin MMC, Mitcheson PD, Green TC. Power loss and thermal characterization of IGBT modules in the alternate arm converter. In: Energy conversion congress exposition (ECCE), Denver, USA. p. 1725–31.
[33] Davies M, Dommaschk M, Dorn J, Lang J, Retzmann D, Soerangr D. HVDC PLUS – basics and principle of operation. Siemens Tech. Rep.; 2008.
[34] Li X, Song Q, Liu W, Rao H, Xu S, Li L. Protection of nonpermanent faults on DC overhead lines in MMC-Based HVDC systems. IEEE Trans Power Deliv 2013;28(1):483–90.
[35] Wang P, Zhang X-P, Deng N, Coventry PF, Zhang R. Control and protection sequence of an offshore integrated MMC MTDC system with master-slave/droop control under converter AC-side fault. In: 6th International conference on advanced power system auto protection (APAP 2015), Nanjing, China. p. 1–5.